Springer

Dear Author,

Here are the proofs of your article.

- You can submit your corrections **online**, via **e-mail** or by **fax**.
- For **online** submission please insert your corrections in the online correction form. Always indicate the line number to which the correction refers.
- You can also insert your corrections in the proof PDF and **email** the annotated PDF.
- For fax submission, please ensure that your corrections are clearly legible. Use a fine black pen and write the correction in the margin, not too close to the edge of the page.
- Remember to note the **journal title**, **article number**, and **your name** when sending your response via e-mail or fax.
- **Check** the metadata sheet to make sure that the header information, especially author names and the corresponding affiliations are correctly shown.
- **Check** the questions that may have arisen during copy editing and insert your answers/ corrections.
- **Check** that the text is complete and that all figures, tables and their legends are included. Also check the accuracy of special characters, equations, and electronic supplementary material if applicable. If necessary refer to the *Edited manuscript*.
- The publication of inaccurate data such as dosages and units can have serious consequences. Please take particular care that all such details are correct.
- Please **do not** make changes that involve only matters of style. We have generally introduced forms that follow the journal's style.
  Substantial changes in content, e.g., new results, corrected values, title and authorship are not allowed without the approval of the responsible editor. In such a case, please contact the Editorial Office and return his/her consent together with the proof.
- If we do not receive your corrections **within 48 hours**, we will send you a reminder.
- Your article will be published **Online First** approximately one week after receipt of your corrected proofs. This is the **official first publication** citable with the DOI. **Further changes are, therefore, not possible.**
- The **printed version** will follow in a forthcoming issue.

Please note

After online publication, subscribers (personal/institutional) to this journal will have access to the complete article via the DOI using the URL: http://dx.doi.org/[DOI].
If you would like to know when your article has been published online, take advantage of our free alert service. For registration and further information go to: http://www.link.springer.com.

Due to the electronic nature of the procedure, the manuscript and the original figures will only be returned to you on special request. When you return your corrections, please inform us if you would like to have these documents returned.

Metadata of the article that will be visualized in OnlineFirst

ArticleTitle	New understanding of the shape-memory response in thiol-epoxy click systems: towards controlling the recovery process	
Article Sub-Title		
Article CopyRight	Springer Science+Business Media New York (This will be the copyright line in the final PDF)	
Journal Name	Journal of Materials Science	
Corresponding Author	Family Name	**Flor**
	Particle	**De la**
	Given Name	**Silvia**
	Suffix	
	Division	Department of Mechanical Engineering
	Organization	Universitat Rovira I Virgili
	Address	Campus Sescelades, Av. dels Països Catalans, 26, 43007, Tarragona, Spain
	Phone	0034-977558839
	Fax	
	Email	silvia.delaflor@urv.net
	URL	
	ORCID	http://orcid.org/0000-0002-6851-1371
Author	Family Name	**Belmonte**
	Particle	
	Given Name	**Alberto**
	Suffix	
	Division	Department of Mechanical Engineering
	Organization	Universitat Rovira I Virgili
	Address	Campus Sescelades, Av. dels Països Catalans, 26, 43007, Tarragona, Spain
	Phone	
	Fax	
	Email	
	URL	
	ORCID	
Author	Family Name	**Fernández-Francos**
	Particle	
	Given Name	**Xavier**
	Suffix	
	Division	Thermodynamics Laboratory
	Organization	ETSEIB, Universitat Politècnica de Catalunya
	Address	Av. Diagonal 647, 08028, Barcelona, Spain
	Phone	
	Fax	
	Email	
	URL	

ORCID

Schedule

Received 11 July 2016

Revised

Accepted 28 September 2016

Abstract

Our research group has recently found excellent shape-memory response in “thiol-epoxy” thermosets obtained with click-chemistry. In this study, we use their well-designed, homogeneous and tailorable network structures to investigate parameters for better control of the shape-recovery process. We present a new methodology to analyse the shape-recovery process, enabling easy and efficient comparison of shape-memory experiments on the programming conditions. Shape-memory experiments at different programming conditions have been carried out to that end. Additionally, the programming process has been extensively analysed in uniaxial tensile experiments at different shape-memory testing temperatures. The results showed that the shape-memory response for a specific operational design can be optimized by choosing the correct programming conditions and accurately designing the network structure. When programming at a high temperature ($T \gg T_g$), under high network mobility conditions, high shape-recovery ratios and homogeneous shape-recovery processes are obtained for the network structure and the programmed strain level (ε_D). However, considerably lower stress and strain levels can be achieved. Meanwhile, when programming at temperatures lower than T_g, considerably higher stress and strain levels are attained but under low network mobility conditions. The shape-recovery process heavily depends on both the network structure and ε_D. Network relaxation occurs during the loading stage, resulting in a noticeable decrease in the shape-recovery rate as ε_D increases. Moreover, at a certain level of strain, permanent and non-recoverable deformations may occur, impeding the completion and modifying the whole path of the shape-recovery process.

Footnote Information

_2D materials
_*ab initio* calculations
_additive manufacturing
_adhesion
_adsorption
_aerogels
_AFM
_alloys
_amorphous materials
_annealing
_antifouling materials
_atomic-layer deposition (ALD)
_atomistic modeling
_batteries
_batteries, lithium
_batteries, magnesium
_batteries, sodium
_BCC metals
_bio-inspired materials
_biomass conversion
_biomaterials
_biomechanics
_biomimetic
_black phosphorus
_blends
_brazing
_calcification
_capacitors
_carbon fiber
_carbon nanotube
_casting
_catalysts or catalysis
_cellular materials
_cellulose
_ceramics
_characterization methods
_chemical vapor deposition (CVD)
_CO_2 sequestration
_coatings
_colloids or bio-colloids
_composite materials
_computational materials science
_computer modeling
_computer simulation
_conducting polymers
_corrosion and oxidation
_corrosion protection
_crystal plasticity
_crystallization
_curing
_data analytics
_defects
_deformation
_deposition
_dielectrics
_diffraction, electron
_diffraction, neutron
_diffraction, X-ray (XRD)
_diffusion
_diodes
_dislocation dynamics
_dislocations
_drug delivery
_dye-sensitized solar cells (DSSCs)
_dysfunctional materials
_EBSD
_elastic properties
_electrical properties
_electrocatalysis
_electrochemistry
_electrode materials
_electron-beam melting
_electronic materials
_electronic properties
_electrospinning
_embrittlement
_energy harvesting
_epitactic or epitaxial growth
_fatigue
_FCC metals
_ferroelectrics
_FGMs
_fibers or fiber technology
_food colloids
_fracture
_fuel cells
_functional anisotropy
_functional materials
_gas-phase transport
_gelation
_geocomposites
_glass
_grain boundaries
_grain boundary engineering
_graphene
_graphitic carbon
_hardness
_HCP metals
_healing
_heat treatment
_hierarchical materials
_high entropy alloys
_high pressure torsion
_high throughput testing
_hot isostatic pressing
_hydrogels
_hydrogen storage or production
_hydrolysis
_II-VI compounds
_III-V compounds
_imaging
_In situ or operando
_infrared spectroscopy
_intercalation
_interfaces
_intermetallics
_ionomers
_kinetics
_laminates
_laser processing
_latticed effects
_layered materials
_light alloys
_light-emitting diodes
_liquid crystals
_lithography
_machining
_macro defects
_magnetic materials or properties
_magnetic ordering
_materials design
_materials for demanding environments
_materials for energy
_mechanical properties
_membranes
_mesoporous materials
_metal-insulator transition
_metal/organic frameworks (MOFs)
_metallic glasses
_metals
_metamaterials
_microanalysis
_microstructure
_minerals or mineralization
_molding
_molecular dynamics
_molecular simulation
_molecular-beam epitaxy (MBE)
_morphology
_multiferroics
_multilayers
_nanocomposites
_nanofunctionality
_nanoindentation
_nanolithography
_nanomaterials
_nanomedicines
_nanoporous materials
_natural materials
_NDT
_NMR
_nuclear materials
_nucleation
_omniphobic materials
_optical materials and properties
_organic electronics
_organic solar-cell materials
_permselective materials
_perovskite
_perovskite solar cell (PSCs)
_phase diagrams
_phase transformations
_phase-change materials (PCMs)
_phase-field modeling
_phosphors
_photocatalysis
_photonic materials
_photoreactive materials
_phototherapeutics
_photovoltaics (solar cells)
_piezoelectric materials
_plasma deposition
_plasmonic materials
_plating
_polymers
_porous materials
_powder technology
_pyroelectrics
_quasicrystals
_radiation damage
_radiation effects
_rapidly solidified materials
_redox flow batteries
_regenerative medicine
_resorbable materials
_responsive materials
_rheology
_sapphire/Al_2O_3
_scaffolds
_scanned-probe microcopy
_selective laser melting
_self-assembly
_self-healing materials
_SEM
_semiconductors
_sensing and sensors
_severe plastic deformation
_shape memory materials
_silicones
_singlet-exciton fission
_sintering
_small volume testing
_smart materials
_sodium-sulphur batteries
_soft interfaces
_soft matter
_sol-gel preparation
_solidification
_solvothermal/hydrothermal
_spectroscopy (XPS)
_spin glass
_spintronics
_sputter deposition
_STM
_superalloys
_supercapacitors
_superconductors
_superelasticity
_superhydrophobic
_surface treatments
_surfaces
_surfactants
_technical textiles
_TEM
_texture
_theranostics
_thermal barrier coatings
_thermal properties
_thermodynamics
_thermoelectrics
_thin-film or thick-film coatings
_TiO_2 rutile, anatase or brookite
_tissue engineering
_tomography
_topological insulators
_transparent conductors
_transport mechanisms
_tribology
_twinning
_TWIP steels
_two-photon adsorption
_UFG materials
_viscoelasticity
_viscosity
_water-splitting
_wear
_wood
_XPS
_zeolite

J Mater Sci

New understanding of the shape-memory response in thiol-epoxy click systems: towards controlling the recovery process

Alberto Belmonte[1], Xavier Fernández-Francos[2], and Silvia De la Flor[1,*]

[1] Department of Mechanical Engineering, Universitat Rovira I Virgili, Campus Sescelades, Av. dels Països Catalans, 26, 43007 Tarragona, Spain

[2] Thermodynamics Laboratory, ETSEIB, Universitat Politècnica de Catalunya, Av. Diagonal 647, 08028 Barcelona, Spain

Received: 11 July 2016
Accepted: 28 September 2016

ABSTRACT

Our research group has recently found excellent shape-memory response in "thiol-epoxy" thermosets obtained with click-chemistry. In this study, we use their well-designed, homogeneous and tailorable network structures to investigate parameters for better control of the shape-recovery process. We present a new methodology to analyse the shape-recovery process, enabling easy and efficient comparison of shape-memory experiments on the programming conditions. Shape-memory experiments at different programming conditions have been carried out to that end. Additionally, the programming process has been extensively analysed in uniaxial tensile experiments at different shape-memory testing temperatures. The results showed that the shape-memory response for a specific operational design can be optimized by choosing the correct programming conditions and accurately designing the network structure. When programming at a high temperature ($T \gg T_g$), under high network mobility conditions, high shape-recovery ratios and homogeneous shape-recovery processes are obtained for the network structure and the programmed strain level (ε_D). However, considerably lower stress and strain levels can be achieved. Meanwhile, when programming at temperatures lower than T_g, considerably higher stress and strain levels are attained but under low network mobility conditions. The shape-recovery process heavily depends on both the network structure and ε_D. Network relaxation occurs during the loading stage, resulting in a noticeable decrease in the shape-recovery rate as ε_D increases. Moreover, at a certain level of strain, permanent and non-recoverable deformations may occur, impeding the completion and modifying the whole path of the shape-recovery process.

Address correspondence to E-mail: silvia.delaflor@urv.net

DOI 10.1007/s10853-016-0456-9

Springer

Journal : 10853 - Large 10853 | Dispatch : 1-10-2016 | Pages : 14
Article No. : 456 | LE | TYPESET
MS Code : JMSC-D-16-03908 | CP | DISK

Introduction

Shape-memory polymers (SMPs) enclose materials capable of storing large strain energy upon external programming (in the form of a temporary-shape), and recovering the original (or releasing the energy stored as mechanical work [1–7]) upon external stimulus (i.e. heat, magnetic field or light) [8–12]. The increasing demand for shape-memory materials for aerospace, structural applications, electronic devices and biomechanical applications (i.e. artificial muscles) has recently redirected the focus to the development of materials with large recoverable deformation limits, high levels of strength, the ability to perform mechanical work (work output) and high resistance to aggressive environments. The easy processing and tailorability of the thermoset-based SMPs make them suitable materials for demanding applications. Specifically, epoxy-based systems are very important not only because of the excellent thermal, chemical and mechanical resistance of the epoxy resin, but mostly because of the great shape-memory capabilities: high stress and strain levels are achieved by properly varying the network structure and accurately choosing the shape-memory programming conditions. Moreover, excellent shape-fixation and shape-recovery performance is achieved by the drastic entropic change that takes place during the glass transition process of these thermosets [13].

In our previous work [14, 15], we developed SMPs based on "click" thiol-epoxy thermosets, and found a promising response for demanding applications (i.e. complex actuators or bio-inspired artificial movements). These materials showed enhanced stress levels in comparison with other epoxy-based SMPs [16] as well as high strain levels. Moreover, it was possible to produce materials with homogeneous network relaxation dynamics, leading to very good shape-memory response. "Click" chemistry is a curing methodology based on the efficiency, versatility and selectivity of the reactions [17]. The thiol-epoxy "click" mechanism is interesting due to the formation of hydroxyl and thioether groups in a single step, which can be further transformed into other polymeric materials [18, 19]. Tertiary amines are commonly used as base catalysts in thiol-epoxy formulations, but their high reactivity makes it difficult to control the reaction. Recently, the use of encapsulated latent imidazoles has been shown to significantly enhance the stability of the uncured mixture [20, 21]. Upon heating, the catalyst is released and the reaction occurs rapidly, resulting in homogeneous and well-defined network structures. This enhances the mechanical properties (strength and deformability) of the shape-memory materials developed [22].

An important issue for the effective application of SMPs is to define suitable operational conditions in order to have a safe and reproducible control of the shape-recovery process. The shape-recovery and -fixation ratios (R_r and R_f) and the shape-recovery rate (V_r) are commonly used parameters for assessment of the shape-memory response. However, the information they provide on the dynamics of the shape-recovery process is limited. In certain applications, such as opening mechanisms for security systems, fast recovery is required once the shape-recovery process is triggered in order to avoid initial and compromising damage to the device, rather than a high R_r at the end. Other applications such as artificial muscles require a high R_r, but control of the whole shape-recovery process is also necessary to properly define the artificial movements. Nevertheless, detailed modelling of the mechanical behaviour of polymers requires time-consuming procedures to give relatively accurate and convincing results that, in addition, are limited to certain experimental conditions [9, 23–25]. More efforts are therefore necessary in order to find methodologies that can easily produce relevant parameters and relationships useful for the specific control of the shape-recovery process.

In this study, we take advantage of the well-defined and tailorable network structures of the thiol-epoxy SMPs, in order to produce materials with different crosslinking densities and network hindrances. Thiol curing agents and epoxy resin monomers with different structures and functionalities were used. In order to investigate the potential capabilities of these shape-memory materials, the study has been divided into an initial analysis of the programming process by uniaxial tensile experiments at room temperature (the temperature at which the temporary-shape is fixed) and at different programming temperatures, followed by the study of the shape-recovery process. The generic ratios R_r, R_f and V_r have been determined and related with stress–strain behaviour under different programming conditions. A new, simple and efficient methodology to analyse the shape-recovery process has also been presented. This methodology is based on a series of mathematical transformations of

Journal : 10853 - Large 10853 Dispatch : 1-10-2016 Pages : 14
Article No. : 456 LE TYPESET
MS Code : JMSC-D-16-03908 CP DISK

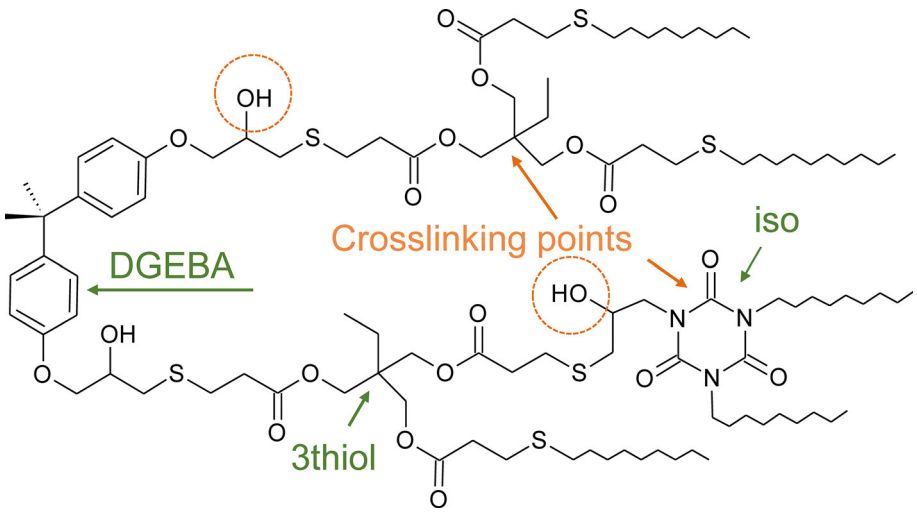

Scheme 1 Expected network structure of the 3thiol-DGEBA-LC80 modified with the *iso* component.

the original data, enabling comparison and analysis of experiments on various materials in terms of the programming conditions. Shape-memory experiments at different programming temperatures and programming strain levels have been carried out and analysed to that end. A more complete understanding of the role of the network structure and programming conditions in the control of the shape-memory response is anticipated, enabling accurate predictions of generic parameters such as R_r, R_f and V_r as well as extensive control of the shape-recovery process. Furthermore, we aim to analyse optimal programming conditions for these promising thiol-epoxy materials in order to strengthen their shape-memory capabilities and broaden their range of application.

Experimental section

Materials

A commercial epoxy resin, Diglycidyl ether of bisphenol A (*DGEBA*, GY240, Huntsman, Everberg, Belgium), with a molecular weight per epoxy equivalent unit of 182 g/equiv. was used as the main epoxy resin. Pentaerythritol tetrakis(3-mercaptopropionate) (4thiol), with a molecular weight per thiol equivalent unit of 122.17 g/equiv. and trimethylolpropane tris(3-mercaptopropionate) (3thiol), with a molecular weight per thiol equivalent unit of 132.85 g/equiv. were used separately as curing agents. In addition, a tris(2,3 epoxypropyl)isocianurate (*iso*), with a molecular weight per epoxy equivalent unit of 99.09 g/equiv. was used as a modifier in a 30 wt% proportion with respect to the total epoxy content (30:70 wt% ISO:DGEBA). The epoxy:thiol equivalent ratio was stoichiometric (1:1). The 3thiol, 4thiol and *iso* were purchased from Sigma-Aldrich, St. Louis, MO, USA). An encapsulated imidazole, 1-methylimidazole (*LC80*, AC Catalysts), was used as a latent initiator at 0.5 parts of catalyst per one hundred parts of epoxy resin (*phr*).

The formulations were prepared by manually stirring the components in a glass vial and carefully pouring the mixtures into an open Teflon mould. The curing process was carried out in an oven, at 120 °C for 1 h, followed by 1 h at 150 °C to allow the completion of the process. Scheme 1 shows the expected network structure after polymerization in mixtures containing iso and 3thiol (the structure using 4thiol would lead to a new chain growing from the fourth arm and the lack of iso in the mixture would be replaced by DGEBA bodies). The crosslinking points and the presence of hydroxyl groups have been highlighted.

Thermo-mechanical properties

The network structure and thermo-mechanical properties of the different materials were studied by dynamic mechanical thermal analysis using a DMA Q800 (TA instrument, New Castle, DE, USA) equipped with a Single-Cantilever (10 mm) clamp. The samples were thoroughly polished to a prismatic rectangular shape ($\approx 20 \times 7.5 \times 1.5$ mm^3) and were analysed at 1 Hz with an oscillation amplitude of 10 μm at a heating rate of 3 °C/min. The T_g was

Journal : 10853 - Large 10853 | Dispatch : 1-10-2016 | Pages : 14
Article No. : 456 | LE | TYPESET
MS Code : JMSC-D-16-03908 | CP | DISK

determined by the peak of the tanδ curve, and the glassy modulus (E_g) and the rubbery modulus (E_r) were determined directly from the storage modulus curve (E). The $T_g^{E'}$ was determined as the onset point of the drop in modulus. The width of the tanδ curve at half-height ($FWHM$) and the tanδ peak were also determined.

The network strand density (v_e) in mol/kg was determined following a modification of the ideal theory of elasticity for elastomeric polymers at low strain rates shown in Eq. (1), defined by the Eq. (2), which takes into account the deviations due to the fluctuations of the functionality of the crosslinking points [26–30].

$$E_r = 3 \cdot R \cdot T \cdot v_e \tag{1}$$

$$v_e = \sum_{f \geq 3} \frac{f-2}{2} \cdot n_f \tag{2}$$

where R is the universal gas constant, T is the temperature at which E_r is determined and n_f is the density of crosslinks with functionality f.

Shape-memory: thermo-mechanical programming characterization

The uniaxial tensile experiments were carried out at the different testing temperatures. The DMA Q800 equipped with a Tension-Film clamp was used to perform the experiments at $T_g^{E'}$, T_g and $T_g + 20$ at a controlled-force rate of 3 N/min. Due to the force limitations of the DMA, an electromechanical universal testing machine (Hounsfield H 10 k-S) with specially designed grips was used to perform the experiments at T_{room}. For the DMA experiments, the samples were thoroughly polished until a dog-bone shape of 15 × 1.4 × 0.5 mm^3 (length × width × thickness) was obtained. For the experiments at room temperature, the size of the specimens was adapted from ASTMD638 requirements, adopting a Type IV dog-bone shape. All the experiments were performed at a crosshead speed of 1 mm/min.

From the σ–ε curves, the stress and strain at break values (σ_b and ε_b respectively) were determined as the failure point of the curves, and the mean value of at least three different samples was reported. The tensile elastic modulus (E_t) was determined as the slope of the curve at the initial and proportional part of the curve.

Shape-memory: response

The shape-memory response was analysed using the DMA Q800 equipped with a Tension-Film clamp in the controlled-force mode. The experiments were carried out as explained in our previous study [14]: first, the sample was heated up to the programming temperature (in accordance with the mechanical analysis, different T_{prog} were chosen: $T_g^{E'}$, T_g and $T_g + 20$). After 5 min of temperature stabilization, the sample was loaded at 3 N/min using a controlled-force ramp until a strain level ε_D equal to 75 % of ε_b was reached (some additional experiments were carried out at ε_D = 15, 30 and 50 % of ε_b when specified). At this point, the sample was rapidly cooled down to T_{room} while maintaining the force applied (the holding time at T_{prog} has been reduced to "0" in order to avoid creep processes affecting the shape-memory response [31]). The sample was then unloaded at the same force rate (3 N/min) and the temporary-shape was fixed. Afterwards, a temperature ramp of 3 °C/min was imposed until the shape-recovery was completed. All the experiments were repeated three times to ensure reproducible results, and the mean value has been presented.

The shape-fixation and shape-recovery ratios were quantified using common expressions; see Eqs. (3) and (4).

$$R_f = \left(\frac{\varepsilon_U}{\varepsilon_D}\right) \cdot 100 \tag{3}$$

$$R_r = \left(\frac{\varepsilon_{D-}\varepsilon_P}{\varepsilon_D}\right) \cdot 100 \tag{4}$$

where R_f is the shape-fixation ratio, R_r is the shape-recovery ratio, ε_D is the programmed strain level (defined as a % of the strain at break, ε_b), ε_U is the remaining strain after unloading and ε_P is the permanent strain after the shape-recovery process takes place. It must be acknowledged that the time after programming and before the recovery-process begins is not taken into account. During this period of time, shape-recovery may take place slowly depending on the programming conditions [32]. In the present study, the temperature ramp begins just after unloading, and there is indeed some time elapsed during heating before the recovery starts, but this time depends on the T_g of the material and would be also affected by the temperature increase. Therefore, in this study, we have chosen to overestimate the

Journal : 10853 - Large 10853 Dispatch : 1-10-2016 Pages : 14
Article No. : 456 LE TYPESET
MS Code : JMSC-D-16-03908 CP DISK

shape-recovery ratio using Eq. (4), taking into consideration the overall process from ε_D to ε_P. The shape-recovery rate (V_r) was quantified from 15 to 85 % of the shape-recovery process as a measure of the average shape-recovery speed; see Eq. (5). Table 1

$$V_r(\%/\text{min}) = \frac{\Delta\%_{SR}}{\Delta t_{\Delta\%SR}} \quad (5)$$

where SR refers to the shape-recovery curve normalized to ε_U. $\Delta\%_{SR}$ is the chosen shape-recovery range (in this case it is from 15 to 85 %, that is, 70 %), and $\Delta t_{\Delta\%SR}$ is the time elapsed from 15 to 85 % of SR.

In order to analyse and compare the shape-recovery process in different formulations and experiments, the shape-recovery curves have been differentiated and normalized as illustrated in Fig. 1. These transformations allow us to properly compare different formulations in terms of the programming conditions. In Fig. 1b, SR is the normalized shape-recovery curve (0 means no recovery, 1 means that the shape-recovery is completed). The curves were normalized to their ε_P, and thus 1 does not mean full-recovery of the original shape but the completion of the shape-recovery process. In Fig. 1c, the shape-recovery speed is defined as $\partial SR/\partial T$ (%/ °C) as a measure of the instantaneous recovery rate [33].

Table 1 Composition of the different formulations of study in wt%

Formulation	DGEBA (wt%)	Thiol (wt%)	*Iso* (wt%)	LC80 (wt%)
3thiol-NEAT	57.64	42.07	0.00	0.29
3thiol-(30 %)iso	36.49	47.61	15.64	0.26
4thiol-NEAT	59.66	40.04	0.00	0.30
4thiol-(30 %)iso	37.95	45.52	16.26	0.27

Results and discussion

Thermo-mechanical properties

The results of the thermo-dynamo-mechanical analysis are shown in Fig. 2 and the parameters of interest are listed in Table 2.

The results of the dynamic mechanical thermal analysis were thoroughly discussed in our previous work [14]. By using curing agents with a different functionality but a similar structure (3thiol and 4thiol) and the mixture of rigid epoxy resins of different functionality and structure (DGEBA and *iso*), it was possible to obtain materials with a homogeneous

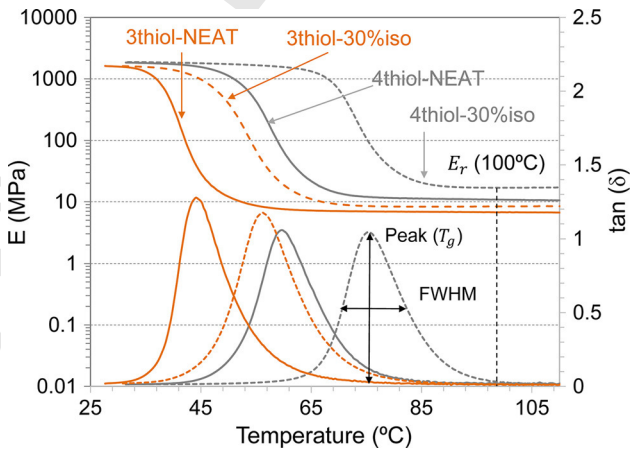

Figure 2 Dynamic mechanical thermal analysis of the different formulations of study. The relaxed modulus (E_r) determination has been *highlighted*.

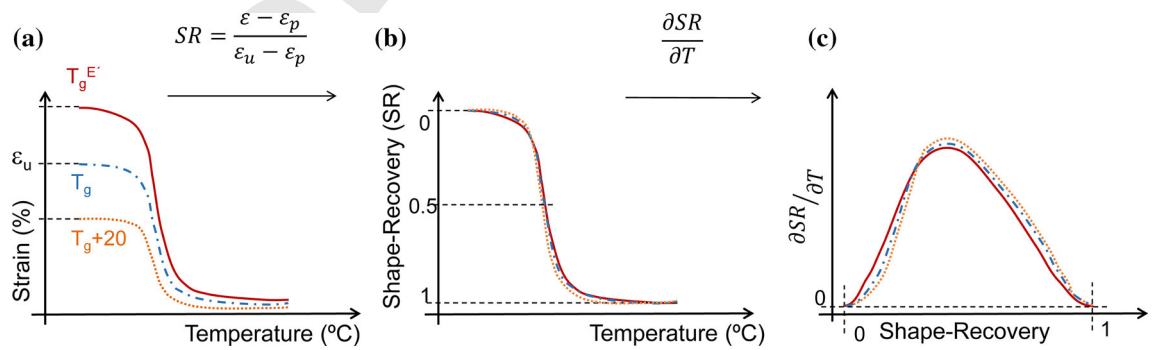

Figure 1 Illustration of the mathematical transformation of the shape-recovery curves. "$\partial SR/\partial T$" is the derivative of the shape-recovery process over the temperature.

Journal : 10853 - Large 10853 | Dispatch : 1-10-2016 | Pages : 14
Article No. : 456 | LE | TYPESET
MS Code : JMSC-D-16-03908 | CP | DISK

Table 2 Network structure and thermo-mechanical properties of the different formulations of study

	3Thiol-NEAT	3Thiol-30 % *iso*	4Thiol-NEAT	4Thiol-30 % *iso*
T_g (°C)	44.1	56.2	59.7	75.4
$T_g^{E'}$(°C)	37.7	46.6	52.0	68.2
FWHM (°C)	10.3	12.5	12.0	11.8
tanδ peak	1.28	1.18	1.06	1.05
E_r (MPa)	6.7	8.5	10.8	17.0
v_e^a (mol/kg)	0.530	0.8633	0.822	1.209

[a] Calculated using Eq. (2)

and tailorable network structure (T_g values ranging from 44.1 to 75.4 °C and rubbery modulus ranging from 6.7 to 17.0 MPa), as well as a narrow and steep relaxation process (low values of FWHM and high values of tanδ peak). The increased functionality in the system leads to a higher crosslinking density and to the formation of more hindered network structures. Systems containing 4thiol instead of 3thiol therefore showed higher T_g and crosslinking density values (see T_g and v_e in Table 2). On the other hand, introducing the isocyanurate in the system increases the functionality, as well as incorporates different types of crosslinking points. The increase in the functionality leads as expected to higher values of T_g and crosslinking density, but the presence of crosslinks of different masses, sizes and rigidities leads to some incompatibilities when the amount of *iso* is too high (>30 %). This phenomenon is more relevant in the case of the 3thiol systems, probably as a result of the presence of an ethyl side chain in the 3thiol structure, which leads to a more heterogeneous and less packed network structure.

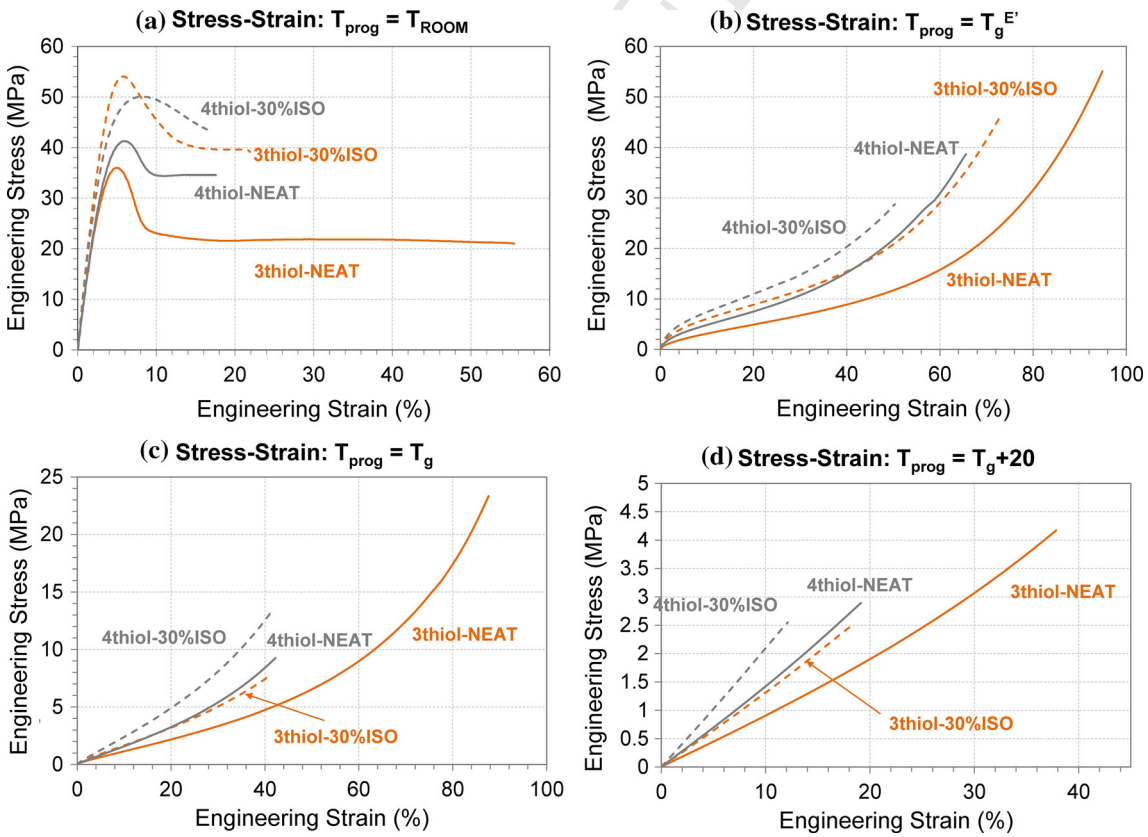

Figure 3 Stress–strain curves for the different formulations of study at the shape-memory testing temperatures; **a** at room temperature; **b** at $T_g^{E'}$; **c** at T_g; **d** at $T_g + 20$.

Journal : 10853 - Large 10853 Dispatch : 1-10-2016 Pages : 14
Article No. : 456 LE TYPESET
MS Code : JMSC-D-16-03908 CP DISK

Table 3 Stress and strain at break values (σ_b and ε_b respectively), tensile elastic modulus (E_t) and the shape-recovery ratio (R_r) at the shape-memory testing temperatures (T_{room}, $T_g^{E'}$, T_g and $T_g + 20$) of the different formulations of study programmed at $\varepsilon_D = 75$ %

	T_{room}			$T_g^{E'}$			T_g			$T_g + 20$		
	σ_b (MPa)	ε_b (%)	E_t (MPa)	σ_b (MPa)	ε_b (%)	R_r (%)	σ_b (MPa)	ε_b (%)	R_r (%)	σ_b (MPa)	ε_b (%)	R_r (%)
3thiol-NEAT	21.0	55.5	1056	55.0	94.9	92.6	23.3	87.6	89.2	4.17	37.8	96.8
3thiol-(30 %)iso	37.6	22.9	1248	46.4	73.1	82.9	7.8	41.5	96.9	2.46	18.1	97.6
4thiol-NEAT	35.7	17.6	1145	38.7	65.6	92.8	9.3	42.2	96.6	2.89	19.1	96.8
4thiol-(30 %)iso	47.0	15.5	1353	28.8	50.3	88.7	13.2	41.2	89.2	2.55	12.1	97.1

The mean value of three different samples tested is shown

Standard deviation of ±0.2 on the stress and strain at break values, ±30 MPa on the elastic modulus at T_{room} ±1 % on the R_r

Shape-memory characterization

The data obtained from the uniaxial tensile experiments (σ–ε curves) at the different shape-memory testing temperatures are shown in Fig. 3: at room temperature T_{room} (the temperature at which the temporary-shape is fixed), at $T_g^{E'}$, T_g and at $T_g + 20$ (the programming temperatures). The stress and strain at break values achieved are summarized in Table 3. For comparison purposes, the shape-recovery ratios, R_r, of the shape-memory experiments carried out at the corresponding programming temperatures and up to $\varepsilon_D = 75$ % are also shown in Table 3.

First of all, as explained in our previous work [14], the optimal mechanical point was found at $T_g^{E'}$, in which both the stress and strain at break values were enhanced, a physical effect called viscoelastic toughening [34, 35]. Moreover, the values obtained are higher than those reported by other authors with epoxy-based systems, especially for the stress at break (up to 55 MPa on the 3thiol-NEAT formulation with 95 % of ε_b at $T_g^{E'}$) [36, 37]. On analysing the σ–ε curves in Fig. 3a, all the formulations were in the glassy state, so that the σ–ε response was similar and only the 3thiol-NEAT formulation differed. The tensile elastic modulus, E_t, is high in all the formulations (around 1 GPa) but the 3thiol-NEAT formulation shows higher ductility (up to 55.5 % of strain at break). This is probably caused by the lower T_g–T_{room} difference and crosslinking density, which enhances the dynamics of the network structure. In terms of shape-memory response, the high elastic modulus and lower ductility of almost all the formulations at room temperature (greater resistance to stretching and hindered mobility of the chains) lead to high shape-fixation (R_f values were almost 100 %) and show that the material is able to maintain the temporary-shape for long periods of time, a useful characteristic for storage purposes, even under constant load (i.e. in certain applications such as security valves, where the temporary-shape is constantly subjected to a pressure until the shape-recovery is triggered).

On analysing the σ–ε curves at the optimal mechanical point, $T_g^{E'}$ (see Fig. 3b), the stress and strain at break values are higher in the case of the 3thiol systems (up to 55 MPa and 95 % respectively). The lower crosslinking density and enhanced mobility of the network chains in the 3thiol systems greatly improve the stress and strain at break values. However, from the change in slope at the beginning of these σ–ε curves, it can be deduced that stress relaxation occurs during this deformation process, because the characteristic relaxation time of the network structure is within and comparable to the time scale of the experiment. Consequently, significant energy losses take place due to viscous friction by network relaxation. Moreover, a strain hardening process is clearly observed at high strain levels in all the formulations studied (mostly in the 3thiol formulations), which may be indicative of damage in the material and a cause of permanent deformation in the network structure after programming the temporary-shape. By contrast, on increasing the temperature to $T_g + 20$ (see Fig. 3d), the network structure relaxation times are highly reduced, and the chains are thus able to quickly reach a stable equilibrium conformational state during loading, with little friction losses. As can be seen in Table 3, the shape-recovery ratio, R_r, in free shape-recovery experiments of samples programmed at $\varepsilon_D = 75$ % considerably

Journal : 10853 - Large 10853 Dispatch : 1-10-2016 Pages : 14
Article No. : 456 LE TYPESET
MS Code : JMSC-D-16-03908 CP DISK

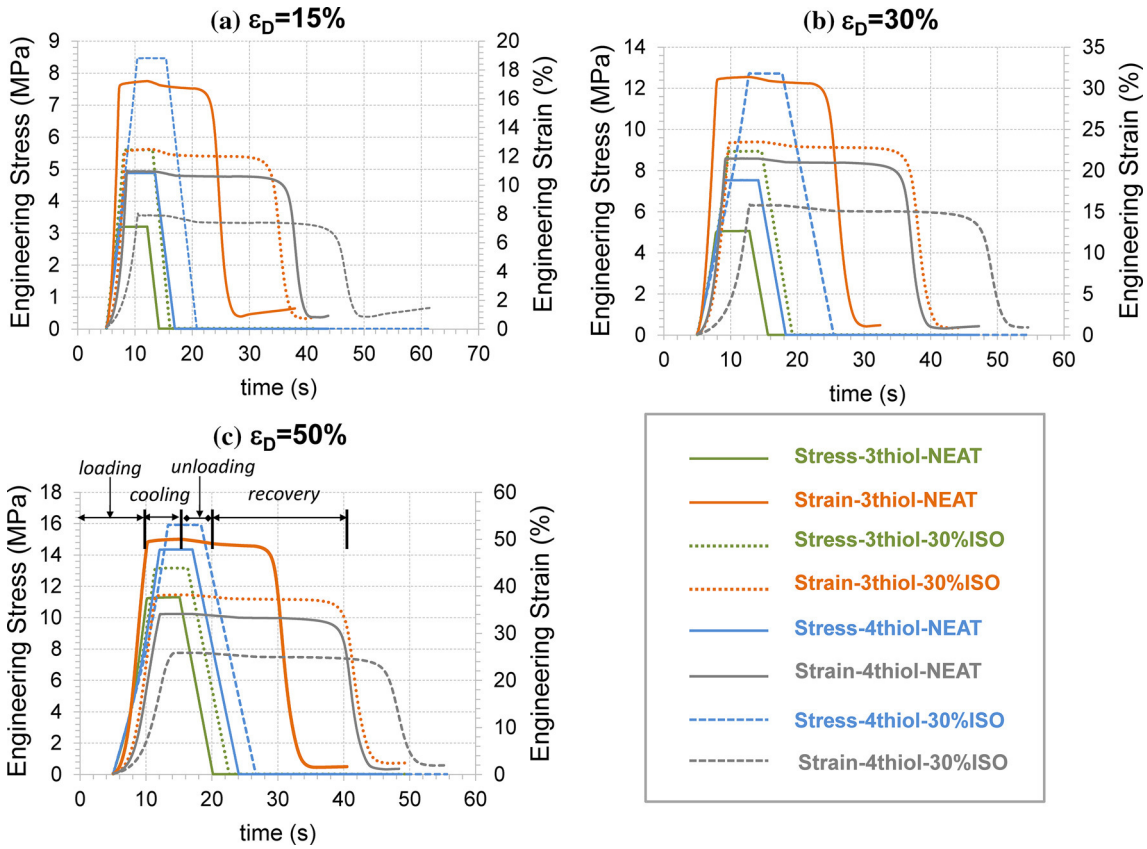

Figure 4 Thermo-mechanical cycles for all the formulations of study programmed at $T_g^{E'}$ and at different strain levels (ε_D = 15, 30 and 50 %).

decreases when T_{prog} decreases from above to below the T_g (i.e. for 3thiol-30 %iso, R_r falls from 97.6 % at $T_g + 20$ to 82.9 % at $T_g^{E'}$, and the same trend is apparent in all the formulations). This could be related to permanent deformation and network damage produced during the loading process at such high deformation levels (higher than the strain at break in the relaxed state), taking place at the same time as the strain hardening that is observed at higher strain levels (see Fig. 3b). In contrast, in those samples programmed at $T_g + 20$, the network structure was already relaxed and therefore under equilibrium conditions during the loading process, leading to no energy losses. The lower strain levels achieved (no strain hardening observed, see Fig. 3d) might have also prevented permanent deformation.

In order to clarify the role of T_{prog} and strain level on the shape-recovery performance, shape-memory experiments were carried out at $T_g^{E'}$, at the same loading rate (1 N/min), but at different programming strain levels (ε_D = 15, 30 and 50 %). The thermo-mechanical cycles for all the experiments performed are presented in Fig. 4 in combined stress-time and strain–time graphs. In Fig. 5, the thermo-mechanical cycles performed at ε_D = 75 % and different T_{prog} are also represented in combined stress-time and strain–time graphs. The shape-recovery ratios, R_r, and shape-recovery rates, V_r, obtained are presented in Table 4 (the results obtained at ε_D = 75 % have been also included for comparison purposes) and are shown in Fig. 6. As it can be seen, R_r is highly enhanced at low strain levels (almost constant and nearly 100 %) while it suddenly decreases at a certain strain level in all the formulations studied. This means that the energy lost due to viscous friction during network relaxation plays a minor role in terms of maximum recoverable strain (R_r), and therefore the lower recovery ratio R_r is probably caused by the damaging processes and permanent deformation taking place during the loading process. The shape-recovery rate V_r of the samples programmed at $T_g^{E'}$ also follows a decreasing trend as ε_D increases, but this can be interpreted in terms of the network relaxation dynamics during the

Journal : 10853 - Large 10853 Dispatch : 1-10-2016 Pages : 14
Article No. : 456 LE TYPESET
MS Code : JMSC-D-16-03908 CP DISK

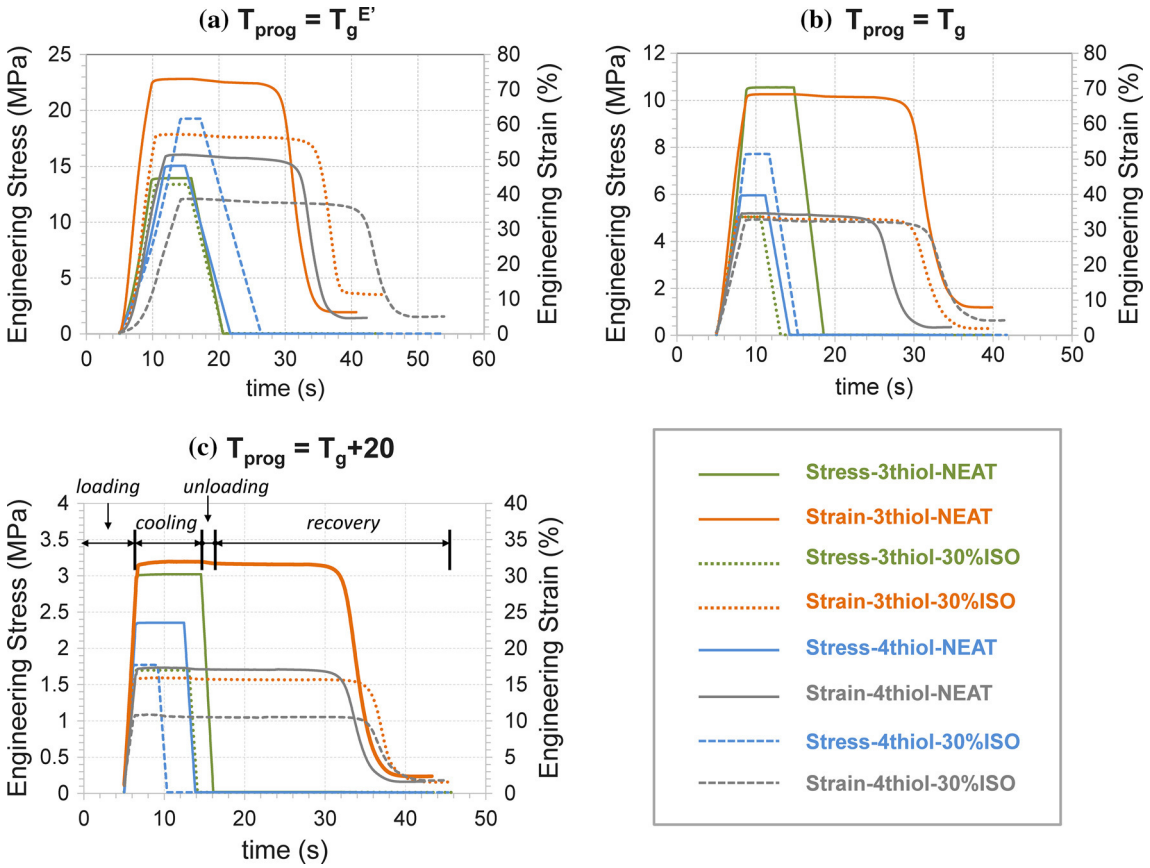

Figure 5 Thermo-mechanical cycles for all the formulations of study programmed at $\varepsilon_D = 75$ % and at programming temperatures ($T_g^{E'}$, T_g and $T_g + 20$).

Table 4 Shape-recovery ratio (R_r) and shape-recovery rate (V_r) as a function of the programming temperature and strain level

T_{prog}		$T_g^{E'}$				T_g	$T_g + 20$
ε_D (%)		15 %	30 %	50 %	75 %[a]	75 %[a]	75 %[a]
3thiol-NEAT	R_r (%)	97.1	97.9	97.5	92.6	89.2	96.8
	V_r (%/min)	33.3	27.8	26.1	22.0	20.1	21.8
3thiol-30 % iso	R_r (%)	96.8	97.5	94.7	83.7	96.9	97.6
	V_r (%/min)	29.2	26.9	24.3	18.9	19.8	26.0
4thiol-NEAT	R_r (%)	97.0	98.3	98.1	92.8	96.6	96.8
	V_r (%/min)	32.6	30.4	26.6	23.3	22.7	23.7
4thiol-30 % iso	R_r (%)	96.5	95.9	94.0	88.7	92.4	97.1
	V_r (%/min)	25.3	23.5	22.3	20.3	21.0	21.8

[a] For comparison purposes, the R_r at $\varepsilon_D = 75$ % have been also included in this table

programming at different ε_D, resulting in materials with different states of network relaxation. In terms of strain recovery velocity, the velocity is higher with increasing strain, but the time required is longer; hence the decrease in the relative recovery rate V_r. The presence of isocyanurate in the network structure tends to decrease R_r and the recovery rate V_r of samples programmed at $T_g^{E'}$, in comparison with the neat formulations, at any ε_D, but especially at $\varepsilon_D = 50$ % and above. This may be due to the presence of isocyanurate, leading to heterogeneities in the network structure resulting in earlier non-recoverable deformations during the loading stage. In addition, experiments at different ε_D were carried out at

Journal : 10853 - Large 10853 Dispatch : 1-10-2016 Pages : 14
Article No. : 456 LE TYPESET
MS Code : JMSC-D-16-03908 CP DISK

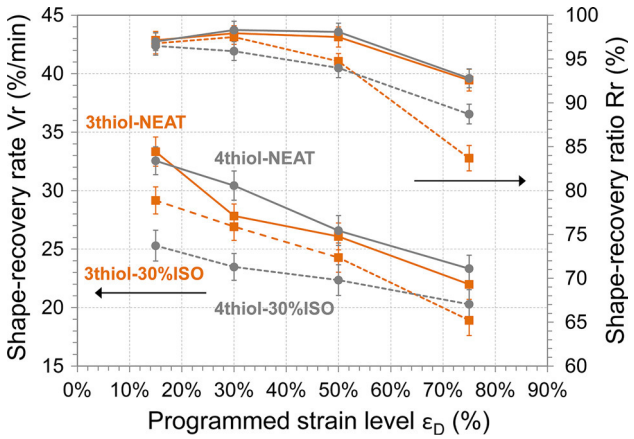

Figure 6 Shape-recovery ratio (R_r) and shape-recovery rate (V_r) for all the formulations of study programmed at $T_g^{E'}$ and at different strain levels.

$T_g + 20$ and these confirmed that the R_r obtained were almost 100 % because the strain levels were moderate and there was therefore no damage in the network structure. Likewise, the relative recovery rate V_r regarding ε_D remained almost constant. As explained above, at this temperature, the chains are able to reach a stable configuration during the loading stage, and similar states of network relaxation are therefore eventually achieved.

As explained in the introduction, generic parameters as the shape-recovery ratio or the shape-recovery rate are not sufficient to design shape-memory materials for smart applications in which full control of the shape-recovery process is of high relevance. For this purpose, the shape-recovery process is analysed by means of the mathematical transformations of the original shape-recovery curves (as illustrated in Fig. 1), which enables comparison of experiments in terms of the programming conditions and formulations of study. First of all, the effect of T_{prog} at the same programmed strain level ($\varepsilon_D = 75$ %) is shown in Fig. 7 for all the formulations of study.

Characteristic bell-shaped curves are obtained in all cases, similar to that of the network relaxation

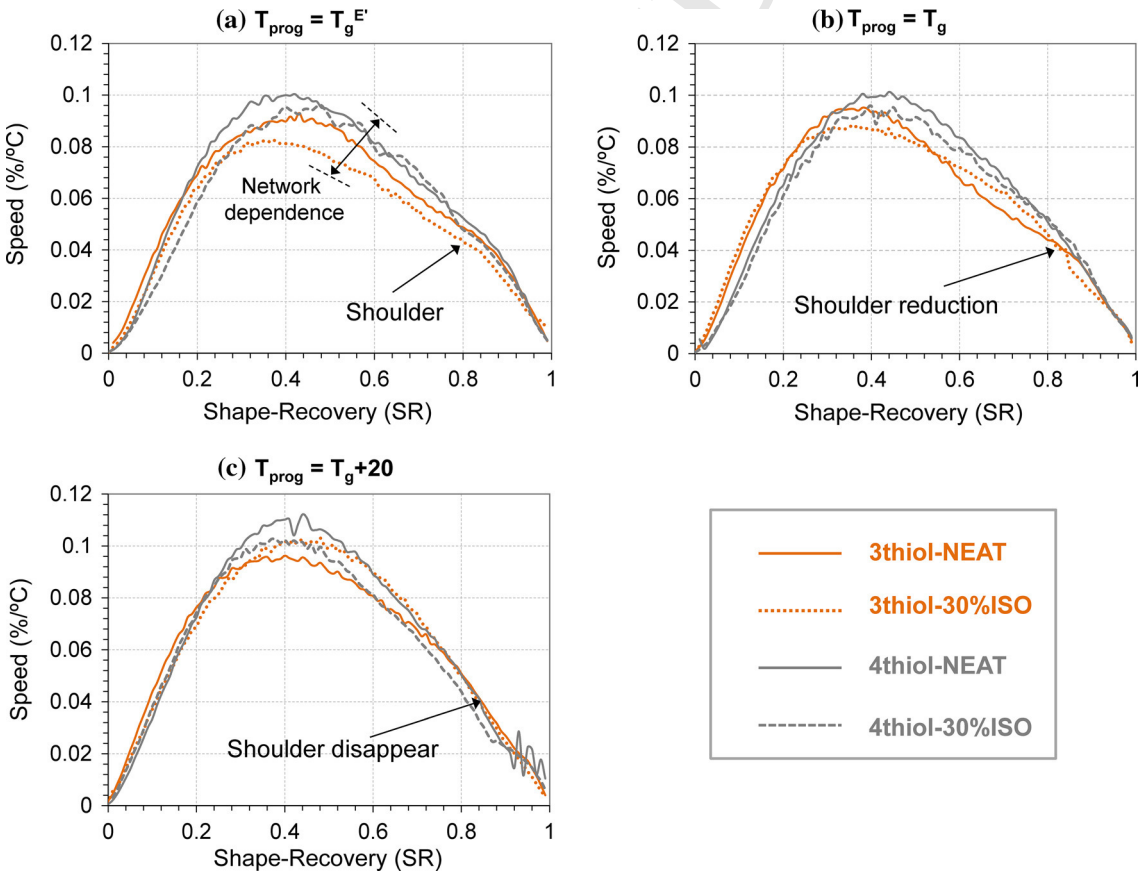

Figure 7 Mathematical transformation of the shape-recovery curves (%/ °C) for all the formulations of study at the different programming temperatures and fixed strain levels ($\varepsilon_D = 75$ %).

Journal : 10853 - Large 10853 | Dispatch : 1-10-2016 | Pages : 14
Article No. : 456 | LE | TYPESET
MS Code : JMSC-D-16-03908 | CP | DISK

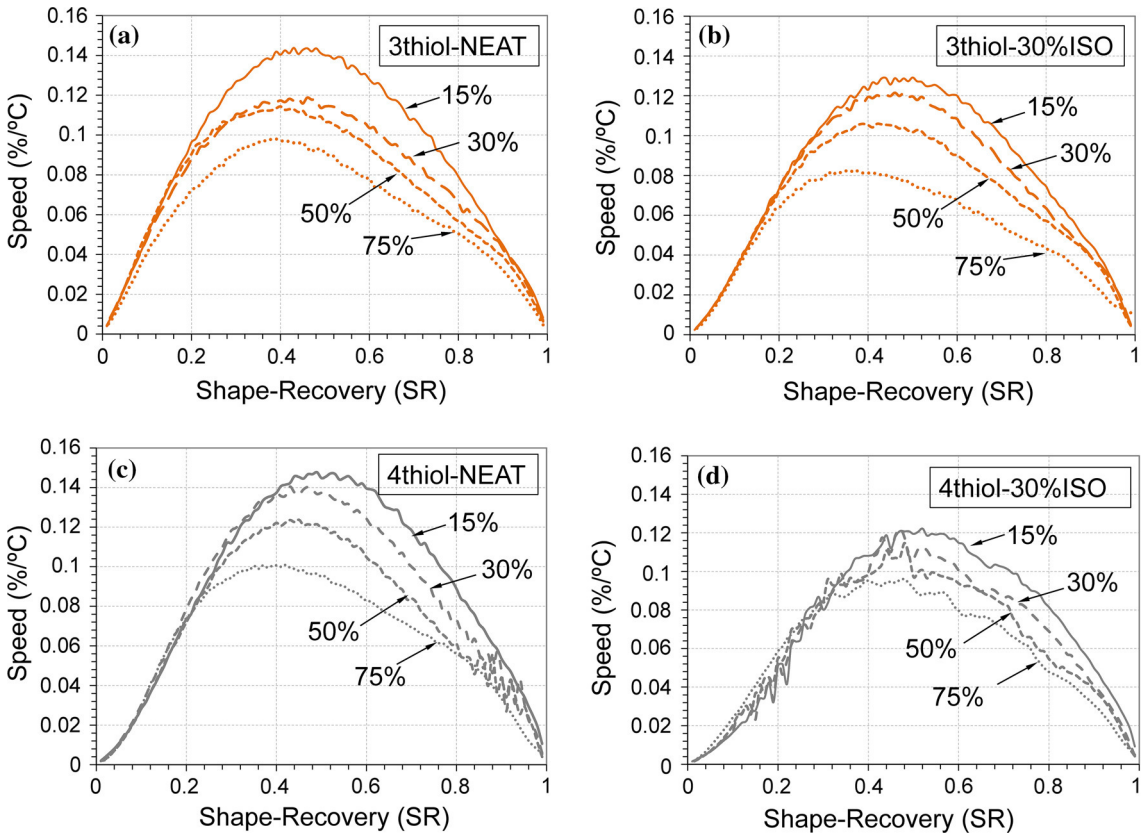

Figure 8 Mathematical transformation of the shape-recovery curves (%/ °C) for all the formulations programmed at $T_g^{E'}$ and at different strain levels (ε_D = 15, 30, 50 and 75 %).

process, but some relevant differences between the different formulations are found. The materials behave in a similar way when programming at $T_g + 20$. At this temperature, the chains easily reach equilibrium during the loading stage, leading to a more stable stretched network architecture as explained above. In consequence, the differences due to the network structure during the shape-recovery process are minimized. However, when programming at $T_g^{E'}$ a noticeable shoulder is appreciated in the final stage of the shape-recovery process. This suggests that the shape-recovery process slows down at some point, but it finally accelerates as the temperature increases. As mentioned above, programming at this temperature, and with such a high level of strain (ε_D = 75 %), may cause some damage to the material, resulting in low shape-memory performance and, in addition, changing the network relaxation dynamics. When programming at higher temperatures, lower strain levels are achieved, and this leads to the progressive disappearance of this shoulder. Some differences are also observed between 3thiol and 4thiol formulations. In 3thiol formulations, the onset of the shape-recovery process is accelerated when programming at T_g and $T_g^{E'}$ and the presence of this shoulder at the end is more evident. As explained previously, this may be due to the presence of a side ethyl chain in the 3thiol systems, which results in a less packed and unstable network structure after programming. This facilitates the beginning of the shape-recovery process [33]. However, differences vanish when programming at $T_g + 20$, indicating that differences in network structure become irrelevant at higher temperatures, from a qualitative point of view.

Using the same methodology, Fig. 8 shows the effect of ε_D on samples programmed at $T_g^{E'}$. It can be observed that the shoulder mentioned above appears at a certain level of strain, while the maximum speed (the peak of the curve) progressively decreases as the strain level ε_D increases. This suggests that the shoulder is mainly related with the damage in the

Journal : 10853 - Large 10853 Dispatch : 1-10-2016 Pages : 14
Article No. : 456 LE TYPESET
MS Code : JMSC-D-16-03908 CP DISK

network structure caused by the strain hardening process at high levels of strain, while the decrease in the maximum speed (which eventually becomes in an overall lowering of the shape-recovery rate, see V_r in Table 4) is mostly related to the increasing viscoelastic recovery time on increasing ε_D due to a change in the network relaxation dynamics.

These results suggest that it is possible to use the high stress levels reached when programming at $T_g^{E'}$ at a certain strain level (i.e. $\varepsilon_D = 50$ %) with no relevant damage in the sample and excellent shape-memory performance: nearly 100 % of R_r and equal or even higher V_r in comparison with that obtained when programming at $T_g + 20$. For example, programming the 3thiol-NEAT formulation at 47.5 % of strain ($\varepsilon_D = 50$ %) leads to around 10 MPa of stress, being both the stress and strain programmed values higher than those reached at $T_g + 20$ (in the 3thiol-NEAT formulation the strain and stress at break values are 37.8 % and around 4 MPa, respectively). This is of crucial importance for applications in which not only enhanced mechanical work is required, but also repeatability without damage is necessary (i.e. in actuators). In this respect, knowledge of the σ–ε programming curves of the shape-memory materials enables a more complete prediction of the shape-recovery process and its performance than when only using common ratios (R_r, R_f and V_r). Through well-designed network structures and properly chosen programming conditions, it is possible to tailor the shape-recovery process as desired: on increasing the programming temperature (or otherwise decreasing the loading rate to allow chains relaxation) the σ–ε curves become flatter, the network structure is able to completely relax the changes induced while the loading process is taking place, minimizing the energy lost due to viscous friction and therefore changes in the network relaxation dynamics, as well as avoiding permanent and non-recoverable deformations in the sample. This leads to high R_r values and more homogeneous shape-recovery processes, but low stress and strain levels are achieved. However, when working at low programming temperatures (in which network relaxation takes place during the loading stage), on increasing the strain level, the energy lost progressively increases due to viscous friction, and damage to the sample may occur, leading to non-recoverable strain (lowering the R_r) and modifying the overall path of the shape-recovery process. In conclusion, it is possible to efficiently optimize the programming conditions in order to adapt the operational design of the shape-memory material to the application requirements.

Conclusions

Materials with homogeneous and well-defined network structures were obtained by a thiol-epoxy "click" reaction catalyzed by latent initiators. From the uniaxial tensile experiments at different T_{prog}, useful predictions of the shape-memory response are possible, not only in terms of common ratios (R_r and R_f) but also of the entire shape-recovery process. The σ–ε curves give us relevant information concerning different stages of the shape-memory response. The high elastic modulus of these materials at the shape-fixation temperature (T_{room}) highlights the good performance in fixing the temporary-shape (R_f was almost 100 %). From the initial change in the slope in the σ–ε curves at the optimal mechanical point ($T_g^{E'} < T_g$), it can be deduced that network relaxation takes place during the loading process, leading to a loss of energy due to viscous friction of the chains. Moreover, at the end of the curves, an increase in the slope shows hardening and therefore damaging processes, which may cause permanent and non-recoverable deformations. The shape-memory experiments show that the network relaxation during programming does not modify the shape-recovery ratio (the sample is able to fully recover its original shape) at moderate strain levels, but decreases the shape-recovery rate V_r. However, exceedingly high programming strain leads to damaging processes, and/or permanent deformations may take place, modifying the whole shape-recovery process and impeding the completion (i.e. low values of R_r). In contrast, when programming at higher temperatures ($T_{prog} \gg T_g$), the curves are flatter and no changes in the slope are appreciated. The chains are able to completely reorganize the changes induced during the loading process, and therefore no network relaxation and energy losses take place. Because of the lower strain level, no permanent or non-recoverable deformation occurs, leading to R_r of nearly 100 % and homogeneous shape-recovery process regardless of the strain level. In addition, the network structure has a minor role at this temperature and there are no differences between formulations.

Journal : 10853 - Large 10853 Dispatch : 1-10-2016 Pages : 14
Article No. : 456 LE TYPESET
MS Code : JMSC-D-16-03908 CP DISK

Nevertheless, the major drawback is the low stress and strain values achieved at this temperature, which may be overcome by well-designed network structure architectures and by an appropriate choice of programming conditions at lower programming temperatures.

Acknowledgements

The authors would like to thank MICINN (MAT2014-53706-C03-01 and MAT2014-53706-C03-02) and Generalitat de Catalunya (2014-SGR-67) for its financial support.

References

[1] Lewis CL, Meng Y, Anthamatten M (2015) Well-defined shape-memory networks with high elastic energy capacity. Macromolecules 48(14):4918–4926

[2] Wang A, Li G (2015) Stress memory of a thermoset shape memory polymer. J Appl Polym Sci 132(24):42112

[3] Arrieta JS, Diani J, Gilormini P (2014) Cyclic and monotonic testing of free and constrained recovery properties of a chemically crosslinked acrylate. J Appl Polym Sci 131(2):39813

[4] Arrieta JS, Diani J, Gilormini P (2014) Experimental characterization and thermoviscoelastic modeling of strain and stress recoveries of an amorphous polymer network. Mech Mater 68:95–103

[5] Anthamatten M, Roddecha S, Li J (2013) Energy storage capacity of shape-memory polymers. Macromolecules 46:42304234

[6] Yakacki CM, Shandas R, Safranski D, Ortega AM, Sassaman K, Gall K (2008) Strong, tailored, biocompatible shape-memory polymer networks. Adv Funct Mater 18:2428–2435

[7] Lakhera N, Yakacki CM, Nguyen TD, Frick CP (2012) Partially constrained recovery of (meth)acrylate shape-memory polymer networks. J Appl Polym Sci 126:72–82

[8] Hager MD, Bode S, Weber C, Schubert US (2015) Shape memory polymers: past, present and future developments. Prog Polym Sci 49–50:3–33

[9] Scalet G, Auricchio F, Bonetti E, Castellani L, Ferri D, Pachera M, Scavello F (2015) An experimental, theoretical and numerical investigation of shape memory polymers. Int J Plast 67:127–147

[10] Lendlein A, Sauter T (2013) Shape-memory effect in polymers. Macromol Chem Phys 214:1175–1177

[11] Anis A, Faiz S, Luqman M, Poulose AM, Gulrez SKH, Shaikh H, Al-Zahrani SM (2013) Developments in shape memory polymeric materials. Polym Plast Technol Eng 52:1574–1589

[12] Habault D, Zhang H, Zhao Y (2013) Light-triggered self-healing and shape-memory polymers. Chem Soc Rev 42:7244–7256

[13] Santhosh Kumar KS, Biju R, Reghunadhan Nair CP (2013) Progress in shape memory epoxy resins. React Funct Polym 73:421–430

[14] Belmonte A, Guzmán D, Fernández-Francos X, De la Flor S (2015) Effect of the network structure and programming temperature on the shape-memory response of thiol-epoxy "click" systems. Polymers 7(10):2146–2164

[15] Belmonte Alberto et al (2016) Network structure dependence on unconstrained isothermal-recovery processes for shape-memory thiol-epoxy "click" systems. Mech Time Depend Mater. doi:10.1007/s11043-016-9322-z

[16] Feldkamp DM, Rousseau IA (2011) Effect of chemical composition on the deformability of shape-memory epoxies. Macromol Mater Eng 296:1128–1141

[17] Binder WH, Sachsenhofer R (2007) "Click" chemistry in polymer and materials science. Macromol Rapid Commun 28:15–54

[18] Carlborg CF, Vastesson A, Liu Y, Van Der Wijngaart W, Johansson M, Haraldsson T (2014) Functional off-stoichiometry thiol-ene-epoxy thermosets featuring temporally controlled curing stages via an UV/UV dual cure process. J Polym Sci 52(2):604–2615

[19] Flores M, Tomuta AM, Fernández-Francos X, Ramis X, Sangermano M, Serra À (2013) A new two-stage curing system: thiol-ene/epoxy homopolymerization using an allyl terminated hyperbranched polyester as reactive modifier. Polymer 54:5473–5481

[20] Guzmán D, Ramis X, Fernández-Francos X, Serra À (2014) New catalysts for diglycidyl ether of bisphenol a curing based on thiol-epoxy click reaction. Eur Polym J. 59:377–396

[21] Brändle A, Khan A (2012) Thiol-epoxy "click" polymerization: efficient construction of reactive and functional polymers. Polym Chem. 3:3224–3227

[22] Berg GJ, McBride MK, Wang C, Bowman CN (2014) New directions in the chemistry of shape memory polymers. Polymer 55:1–24

[23] Xiao R, Guo J, Nguyen TD (2015) Modeling the multiple shape memory effect and temperature memory effect in amorphous polymers. RSC Adv 5:416–423

[24] Barot G, Rao IJ (2006) Constitutive modeling of the mechanics associated with crystallizable shape memory polymers. Zeitschrift Fur Angew Math Und Phys. 57:652–681

Journal : 10853 - Large 10853 | Dispatch : 1-10-2016 | Pages : 14
Article No. : 456 | ☐ LE | ☐ TYPESET
MS Code : JMSC-D-16-03908 | ☑ CP | ☑ DISK

[25] Diani J, Gilormini P, Frédy C, Rousseau IA (2012) Predicting thermal shape memory of crosslinked polymer networks from linear viscoelasticity. Int J Solids Struct 49:793–799

[26] Graessley WW (1975) Statistical Mechanics of Random Coil Networks. Rubber Chem Technol 48:1008–1017

[27] Miller DR, Macosko CW (1976) A new derivation of postgel properties of network polymers. Rubber Chem Technol 49:1219–1231

[28] Charlesworth JM (1988) Effect of crosslink density on molecular relaxations in diepoxide-diamine network polymers. The rubbery plateau region 28:230–236

[29] Lesser A, Crawford E (1997) The role of network architecture on the glass transition temperature of epoxy resins. J Appl Polym Sci 66:387–395

[30] Pascault JP, Sautereau H, Verdu J, Williams RJJ (2002) Thermosetting polymers, 1st edn. CRC Press, New York

[31] Li G, Xu W (2011) Thermomechanical behavior of thermoset shape memory polymer programmed by cold-compression: testing and constitutive modeling. J Mech Phys Solids 59:1231–1250. doi:10.1016/j.jmps.2011.03.001

[32] Li G, Wang A (2016) Cold, warm, and hot programming of shape memory polymers. J Polym Sci 54:1319–1339. doi:10.1002/polb.24041

[33] Pandini S, Bignotti F, Baldi F, Passera S (2013) Network architecture and shape memory behavior of cold-worked epoxies. J Intell Mater Syst Struct 24:1583–1597. doi:10.1177/1045389X13478275

[34] Feldkamp DM, Rousseau IA (2010) Effect of the deformation temperature on the shape-memory behavior of epoxy networks. Macromol Mater Eng 295:726–734

[35] Yakacki CM, Willis S, Luders C, Gall K (2008) Deformation limits in shape-memory polymers. Adv Eng Mater 10:112–119

[36] Leonardi AB, Fasce LA, Zucchi IA, Hoppe CE, Soulé ER, Pérez CJ, Williams JJ (2011) Shape memory epoxies based on networks with chemical and physical crosslinks. Eur Polym J. 47(3):362–369

[37] Santiago D, Fernández-Francos X, Ferrando F, De la Flor S (2015) Shape-memory effect in hyperbranched poly (ethyleneimine)-modified epoxy thermosets. J Polym Sci 53(13): 924–933

Journal : 10853 - Large 10853 | Dispatch : 1-10-2016 | Pages : 14
Article No. : 456 | ☐ LE | ☐ TYPESET
MS Code : JMSC-D-16-03908 | ☑ CP | ☑ DISK

Journal : **10853**
Article : **456**

Springer
the language of science

Author Query Form

Please ensure you fill out your response to the queries raised below and return this form along with your corrections

Author Proof

Dear Author

During the process of typesetting your article, the following queries have arisen. Please check your typeset proof carefully against the queries listed below and mark the necessary changes either directly on the proof/online grid or in the 'Author's response' area provided below

Query	Details Required	Author's Response
AQ1	Table 1 was received: Table 1 has cited manually. Please check and confirm.	
AQ2	Please check and confirm the artwork provided for the Figs. 7 and 8 as two versions have been provided.	